

Copper(II) complexes with N,O-coordinating thiopseudoureas: syntheses, structures, and properties

Kinche Shakunthala, Seema Nagarajan, Gunasekaran Balamurugan & Samudranil Pal

To cite this article: Kinche Shakunthala, Seema Nagarajan, Gunasekaran Balamurugan & Samudranil Pal (2023) Copper(II) complexes with N,O-coordinating thiopseudoureas: syntheses, structures, and properties, Journal of Coordination Chemistry, 76:16-24, 1856-1866, DOI: [10.1080/00958972.2023.2292476](https://doi.org/10.1080/00958972.2023.2292476)

To link to this article: <https://doi.org/10.1080/00958972.2023.2292476>



View supplementary material [↗](#)



Published online: 30 Dec 2023.



Submit your article to this journal [↗](#)



Article views: 19



View related articles [↗](#)



View Crossmark data [↗](#)



Copper(II) complexes with N,O-coordinating thiopseudoureas: syntheses, structures, and properties

Kinche Shakunthala, Seema Nagarajan, Gunasekaran Balamurugan and Samudranil Pal

School of Chemistry, University of Hyderabad, Hyderabad, India

ABSTRACT

Syntheses, characterization, and physical properties of two complexes of copper(II) having the general molecular formula $[\text{Cu}(\text{L}^n)]_2$ (**1** and **2**) with benzyl-*N'*-(4-*R*-benzoyl)-*N*-(2,6-diisopropylphenyl)carbamimidothioates (HL^n , where $n=1$ and 2 for $\text{R}=\text{H}$ and Cl , respectively) are reported. Both complexes were characterized by mass spectrometric, magnetic susceptibility, and various spectroscopic (IR, UV–Vis, and EPR) measurements. The molecular structures of **1** and **2** were established by single crystal X-ray crystallographic studies. In each complex, the bivalent metal center is in a near perfect square-planar $\text{trans-N}_2\text{O}_2$ coordination environment assembled by two bidentate six-membered chelate rings forming iminolate-O and azomethine-N donor $(\text{L}^n)^-$ ligands. In the crystal lattice, the packing of **1** is according to the symmetry operations, while intermolecular $\pi\cdots\pi$ and $\text{C-H}\cdots\pi$ interactions assisted self-assembly of **2** leads to a two-dimensional sheet-like structure. Mass spectrometric and infrared and electronic spectroscopic data are in agreement with their molecular formulas and similar structures. The room temperature magnetic moments and EPR spectra of both complexes are consistent with the $S=1/2$ ground state and the square-planar coordination geometry of the metal ion in each complex.

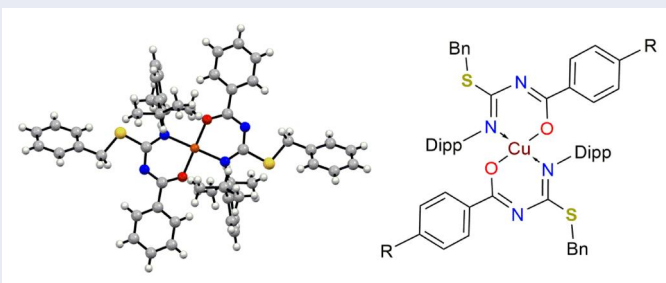
ARTICLE HISTORY

Received 11 September 2023


Accepted 30 November 2023

KEYWORDS

Copper(II) complexes;
thiopseudourea; NO-donor;
crystal structures; properties



CONTACT Samudranil Pal ✉ spal@uohyd.ac.in School of Chemistry, University of Hyderabad, Hyderabad 500046, India

 Supplemental data for this article can be accessed online at publisher's website.

© 2023 Informa UK Limited, trading as Taylor & Francis Group

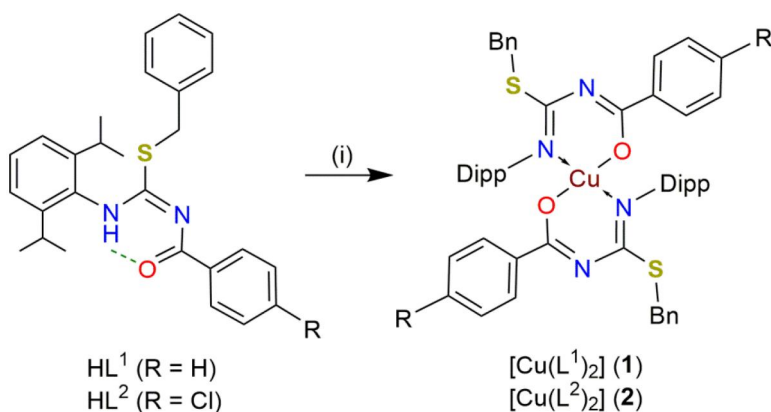
1. Introduction

Thiourea, isothiourea, and thiopseudourea derivatives and their complexes with transition metal ions have attracted interest due to their coordination, catalytic, biological, and biochemical properties. These versatile properties have led to their wide-ranging use as receptors, catalysts in a variety of organic reactions, and pharmaceuticals for therapeutic and diagnostic applications [1–4]. Recently we reported two complexes of nickel(II) having the general formula $[\text{Ni}(\text{L}^n)_2]$ with two thiopseudoureas benzyl-*N'*-(4-*R*-benzoyl)-*N*-(2,6-diisopropylphenyl)carbamimidothioates (HL^n , where $n=1$ and 2 for $\text{R}=\text{H}$ and Cl , respectively) [5]. In these complexes, despite more steric crowding around the N-atom in contrast to the S-atom, the ligand $(\text{L}^n)^-$ is an O,N-donor to nickel(II) instead of O,S-donor both being six-membered chelate rings. The reason behind the observed O,N-coordination mode of $(\text{L}^n)^-$ is the effective delocalization of its negative charge which is not possible in the alternative O,S-coordination mode. Herein, we have investigated the coordination behavior of the above mentioned two thiopseudoureas (HL^n) toward copper(II) and isolated two analogous complexes of formula $[\text{Cu}(\text{L}^n)_2]$ (Scheme 1). Here also, $(\text{L}^n)^-$ is O,N-coordinated to the metal center. In the following sections, we have described the syntheses, X-ray structures, and physical properties of these two complexes.

2. Experimental

2.1. Materials

Benzyl-*N'*-(4-*R*-benzoyl)-*N*-(2,6-diisopropylphenyl)carbamimidothioates (HL^1 and HL^2) were synthesized in high (~90%) yields using the corresponding 4-*R*-benzoyl chlorides ($\text{R}=\text{H}$ and Cl), NH_4SCN , 2,6-diisopropylaniline, and benzyl bromide according to a procedure reported earlier [3(b), 5]. All other chemicals were of reagent grade available commercially and were used as received. Solvents used were purified by standard methods [6].



Scheme 1. Syntheses of $[\text{Cu}(\text{L}^{1/2})_2]$ (1 and 2): (i) $\text{Cu}(\text{OAc})_2 \cdot \text{H}_2\text{O}$ in $\text{MeOH}-\text{CHCl}_3$ (1:1) mixture at 50°C for 24 h.

2.2. Physical measurements

A Bruker Maxis (ESI-TOF analyzer) spectrometer was used to record the mass spectra. Magnetic susceptibility measurements were performed with a Sherwood scientific balance. Diamagnetic corrections calculated from Pascal's constants [7] were used to obtain the molar paramagnetic susceptibilities. Infrared spectra were recorded in ATR mode with a Thermo Scientific Nicolet iS5 FT-IR spectrophotometer. Electronic spectra were recorded using a Shimadzu UV-3600 UV-Vis-NIR spectrophotometer. A Jeol JES-FA200 spectrometer was used to record EPR spectra.

2.3. Synthesis of $[\text{Cu}(\text{L}^1)_2]$ (**1**)

A solution of $\text{Cu}(\text{OAc})_2 \cdot \text{H}_2\text{O}$ (200 mg, 1 mmol) in methanol (30 mL) was added to a chloroform solution (30 mL) of HL^1 (862 mg, 2 mmol), and the mixture was stirred at 50 °C for 24 h. The light green solid separated was collected by filtration, washed with water, and finally dried under vacuum. The dry solid was then recrystallized from a 1:1 mixture of chloroform and methanol. Yield: 600 mg (65%). ESI-MS Data Calcd (found) for $[\mathbf{1} + \text{H}]^+$ (m/z): 922.3370 (922.3253). Selected IR band (cm^{-1}): 1591 (C = N). UV-Vis data in CHCl_3 [λ_{max} (nm) (ϵ ($\text{M}^{-1} \text{cm}^{-1}$))]: 565 (111), 395 (3.7×10^3), 274 (7.6×10^4). μ_{eff} (μ_{B}): 1.71.

2.4. Synthesis of $[\text{Cu}(\text{L}^2)_2]$ (**2**)

Complex **2** was synthesized by following the same procedure as described above for **1** using $\text{Cu}(\text{OAc})_2 \cdot \text{H}_2\text{O}$ (200 mg, 1 mmol) and HL^2 (930 mg, 2 mmol). Yield: 615 mg (62%). ESI-MS Data Calcd (found) for $[\mathbf{2} + \text{H}]^+$ (m/z): 992.2577 (992.2510). Selected IR band (cm^{-1}): 1579 (C = N). UV-Vis data in CHCl_3 [λ_{max} (nm) (ϵ ($\text{M}^{-1} \text{cm}^{-1}$))]: 560^{sh} (139), 398 (5.2×10^3), 283 (10.4×10^4). μ_{eff} (μ_{B}): 1.72.

2.5. X-ray crystallography

X-ray quality single crystals of $[\text{Cu}(\text{L}^1)_2]$ (**1**) and $[\text{Cu}(\text{L}^2)_2]$ (**2**) were grown by slow evaporation of their solutions in chloroform-methanol (1:1) mixture. A Rigaku Oxford XtaLAB Synergy equipped with a HyPix3000 CCD area detector and PhotonJet micro-focus source for mirror monochromated Mo $K\alpha$ radiation ($\lambda = 0.71073 \text{ \AA}$) was used for the unit cell determination and the intensity data collection at 298 K for **1**. Data acquisition, integration, reduction, and absorption correction were performed using CrysAlisPro software package [8]. Unit cell determination and intensity data collection for **2** were carried out at 298 K on a Bruker D8 Quest diffractometer fitted with a Photon 100 CMOS area detector and an Incoatec microfocus source for graphite monochromated Mo $K\alpha$ radiation ($\lambda = 0.71073 \text{ \AA}$). APEX3 software package [9] was used for data acquisition, integration, and reduction. The SADABS program [10] was employed for an empirical absorption correction. Structures of both complexes were solved by direct methods and refined on F^2 using full-matrix least-squares procedures. In each structure, all nonhydrogen atoms were refined with anisotropic displacement parameters and the hydrogen atoms were placed in idealized positions and included

Table 1. Selected crystal data for [Cu(L¹)₂] (**1**) and [Cu(L²)₂] (**2**).

Complex	1	2
Chemical formula	C ₅₄ H ₅₈ N ₄ O ₂ S ₂ Cu	C ₅₄ H ₅₆ N ₄ O ₂ S ₂ Cl ₂ Cu
Formula weight	922.70	991.59
Crystal system	Triclinic	Triclinic
Space group	<i>P</i> $\bar{1}$	<i>P</i> $\bar{1}$
<i>a</i> (Å)	9.34213(19)	8.4568(8)
<i>b</i> (Å)	10.6633(2)	12.5798(14)
<i>c</i> (Å)	13.4522(2)	12.8615(14)
α (°)	68.9231(19)	97.099(4)
β (°)	80.6265(17)	105.585(4)
γ (°)	80.4844(18)	97.431(4)
<i>V</i> (Å ³)	1225.41(4)	1288.8(2)
<i>Z</i>	1	1
ρ (g cm ⁻³)	1.250	1.278
μ (mm ⁻¹)	0.575	0.652
Reflections collected	25,319	41,160
Reflections unique	4305	4522
Reflections $I \geq 2\sigma(I)$	3413	3348
Data/restraints/parameters	4305/0/290	4522/0/295
<i>R</i> 1, <i>wR</i> 2 ($I \geq 2\sigma(I)$)	0.0516, 0.1365	0.0489, 0.1135
<i>R</i> 1, <i>wR</i> 2 (all data)	0.0678, 0.1481	0.0777, 0.1237
GOF on <i>F</i> ²	1.066	1.043
Final diff. peak/hole (e Å ⁻³)	0.396, -0.500	0.342, -0.298

in the refinement by using a riding model. The SHELX-97 programs [11] accessed through the WinGX suite [12] were used for structure solution and refinement. Structural illustrations were prepared using the Mercury package [13]. Selected crystal and refinement data for **1** and **2** are listed in Table 1.

3. Results and discussion

3.1. Synthesis and properties

Reactions of Cu(OAc)₂ · H₂O with HL¹ and HL² in 1:2 mole ratio in MeOH–CHCl₃ (1:1) mixture (Scheme 1) provided [Cu(L¹)₂] (**1**) and [Cu(L²)₂] (**2**), respectively, in good yields (>60%). In the ESI-MS spectra of both complexes, the *m/z* values of the base peaks and their isotopic patterns are in agreement with their corresponding molecular formulas (Figures S1 and S2 in Supplementary Material). The room temperature (30 °C) effective magnetic moments of **1** and **2** are 1.71 and 1.72 μ_B , respectively. These values are consistent with the +2 oxidation state of the metal ion and hence d⁹ electronic configuration ($S = 1/2$). At room temperature, both complexes are insoluble in most common organic solvents such as methanol, ethanol, acetonitrile, dimethylsulfoxide, and *N,N*-dimethylformamide, but they are highly soluble in dichloromethane and chloroform, providing green solutions. In solution, each complex behaves as a nonelectrolyte.

3.2. X-ray structures

The structures of both **1** and **2** have been solved in the triclinic *P* $\bar{1}$ space group. Each of the two complex molecules is centrosymmetric with copper at the inversion center. As a result, the asymmetric unit of each structure contains copper with half occupancy

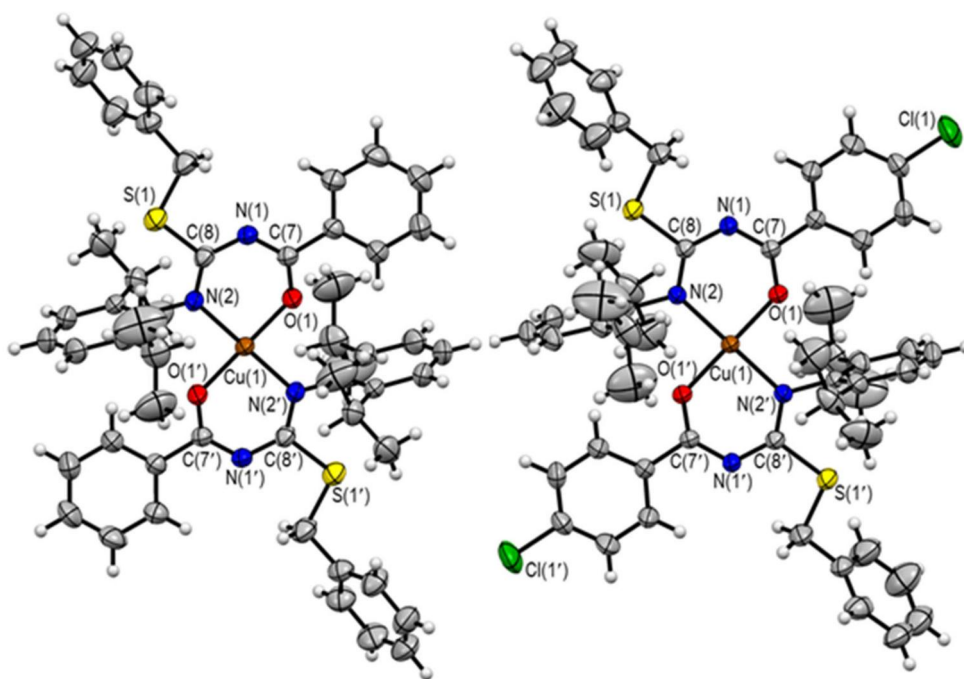


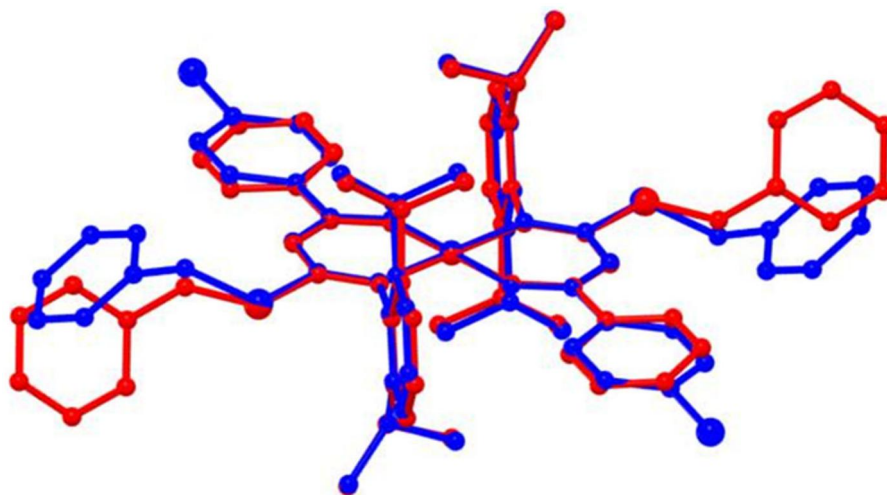
Figure 1. Molecular structures of $[\text{Cu}(\text{L}^1)_2]$ (**1**) (left) and $[\text{Cu}(\text{L}^2)_2]$ (**2**) (right). In both structures, thermal ellipsoids of all nonhydrogen atoms are drawn at 40% probability level and the hydrogen atoms are shown as spheres of arbitrary radius. Only selected atoms of each molecule are labeled for clarity.

and one bidentate ligand $(\text{L}^n)^-$. The molecular structures of **1** and **2** are depicted in [Figure 1](#). Selected bond parameters are listed in [Table 2](#). In both **1** and **2**, C(7)–N(1) bond is $\sim 0.06 \text{ \AA}$ shorter and the C(7)–O(1) bond is $\sim 0.04 \text{ \AA}$ longer in comparison to the corresponding bonds in HL^1 and HL^2 [5]. On the other hand, the C(8)–N(1) bond is $\sim 0.03 \text{ \AA}$ longer and C(8)–N(2) bond is $\sim 0.01 \text{ \AA}$ shorter in **1** and **2** when compared with those bonds in HL^1 and HL^2 [5]. Thus, after deprotonation the amine-imine-ketone ($-\text{N}2(\text{H})-\text{C}8=\text{N}1-\text{C}7(=\text{O}1)-$) fragment of HL^n becomes imine-iminolate ($-\text{N}2=\text{C}8-\text{N}1=\text{C}7(-\text{O}1^-)-$) in the ligand $(\text{L}^n)^-$ of both **1** and **2** ([Scheme 1](#) and [Figure 1](#)). The ligand $(\text{L}^n)^-$ can coordinate a metal ion through the iminolate-O and the azomethine-N atoms or iminolate-O and the thioether-S atoms. Both coordination modes form a six-membered chelate ring. In each of **1** and **2**, the $(\text{L}^n)^-$ has the O,N-coordination mode as observed for the analogous nickel(II) complexes [5]. The O,N-coordination instead of the sterically less crowded O,S-coordination is preferred due to the delocalization of the negative charge, which is possible only in the former mode ([Scheme 1](#) and [Figure 1](#)). In a similar competitive situation, it has been found that copper(II) can have either O,N-coordination [14] or O,S-coordination [1(d), 15] provided the negative charge of the ligand is delocalized. Thus, it appears that the resonance stabilization energy decides the coordination mode of this type of ligand. In both **1** and **2**, the two inverse symmetry related $(\text{L}^n)^-$ assemble an essentially ideal square-planar $\text{trans-N}_2\text{O}_2$ coordination environment where the copper(II) resides at the center of the square-plane. The

Table 2. Selected bond lengths (Å) and angles (°) for **1** and **2**.

Complex	1	2
C(7)–O(1)	1.270(3)	1.268(3)
C(7)–N(1)	1.305(4)	1.310(4)
C(8)–N(1)	1.343(4)	1.344(4)
C(8)–N(2)	1.317(4)	1.313(4)
C(8)–S(1)	1.759(3)	1.764(3)
Cu(1)–O(1)	1.881(2)	1.904(2)
Cu(1)–O(1')	1.881(2)	1.904(2)
Cu(1)–N(2)	1.976(2)	1.967(2)
Cu(1)–N(2')	1.976(2)	1.967(2)
O(1)–Cu(1)–O(1')	180.0	180.0
O(1)–Cu(1)–N(2)	89.93(9)	89.91(9)
O(1)–Cu(1)–N(2')	90.07(9)	90.09(9)
O(1')–Cu(1)–N(2)	90.07(9)	90.09(9)
O(1')–Cu(1)–N(2')	89.93(9)	89.91(9)
N(2)–Cu(1)–N(2')	180.0	180.0(1)

Symmetry transformations used to generate equivalent atoms: **1**: $-x + 1, -y + 1, -z + 1$; **2**: $-x + 1, -y, -z + 1$.

**Figure 2.** A molecular overlay of $[\text{Cu}(\text{L}^1)_2]$ (**1**) (red) and $[\text{Cu}(\text{L}^2)_2]$ (**2**) (blue). Hydrogen atoms are omitted for clarity.

cis angles are within the narrow range of $89.91(9)$ – $90.09(9)^\circ$ and the *trans* angles are 180° with no deviation of any of the atoms from the mean plane constituted by CuN_2O_2 . As a matter of fact, except for the phenyl rings, all the atoms in the two six-membered chelate rings including the thioether-S and the benzylic-C atoms are satisfactorily planar (plane-a) in both complexes (rms deviations: 0.05 and 0.08 Å for **1** and **2**, respectively; Figure 1). As expected, due to the presence of the isopropyl (ip) groups the 2,6-diip-phenyl ring plane (average rms deviation 0.005 Å) and plane-a are very close to orthogonal (dihedral angles are $86.8(1)^\circ$ in **1** and $90.0(1)^\circ$ in **2**). The dihedral angle between plane-a and the benzoyl group phenyl ring planes (average rms deviation 0.007 Å) are also very similar in both **1** ($7.2(2)^\circ$) and **2** ($5.4(2)^\circ$). In contrast, the dihedral angle between plane-a and the benzyl group phenyl ring planes (average rms deviation 0.004 Å) are much larger and quite different in **1** ($58.1(1)^\circ$) and **2** ($70.2(1)^\circ$). The above dihedral angles and the structure overlay diagram (Figure 2)

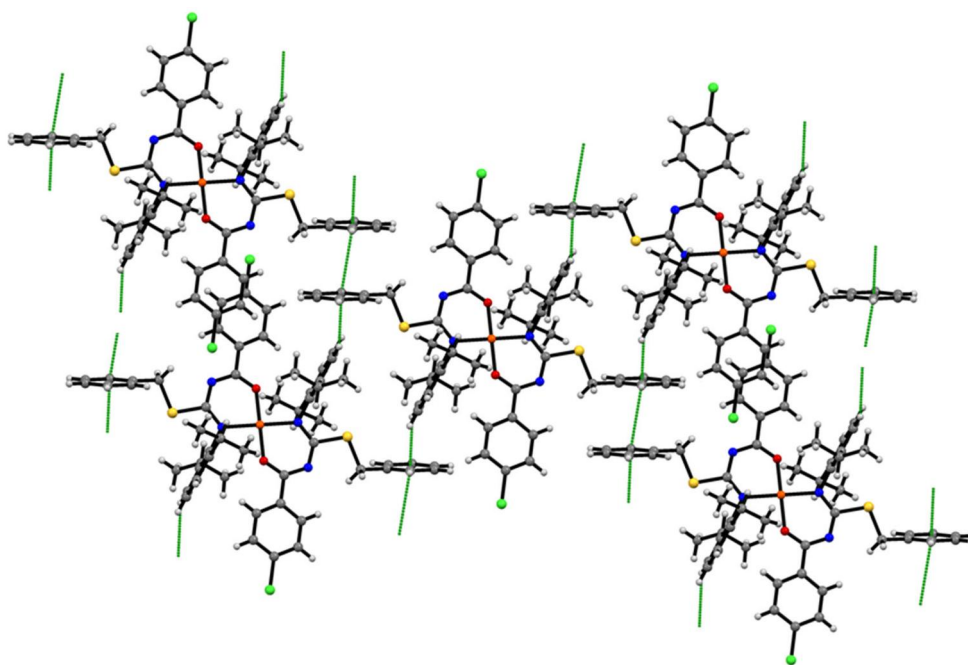


Figure 3. Intermolecular $\pi \cdots \pi$ and C–H $\cdots \pi$ interactions in $[\text{Cu}(\text{L}^2)_2]$ (**2**).

clearly indicate that except for the benzyl groups the remaining portions of the molecules of **1** and **2** are almost superimposable. In general, the Cu–N and Cu–O bond lengths and bond angles in both **1** and **2** are very similar (Table 2) and comparable with those reported for copper(II) square-planar complexes with analogous six-membered chelate ring forming ligands [14].

Both structures have been scrutinized for noncovalent intermolecular interactions to reveal the self-assembly patterns. No significant noncovalent interaction has been found in the case of **1**. Thus, the packing of the molecules in the crystal lattice is guided by the symmetry operations (Figure S3 in Supplementary Material). On the other hand, every molecule of **2** is connected to four neighboring molecules *via* intermolecular $\pi \cdots \pi$ and C–H $\cdots \pi$ interactions involving the benzyl group phenyl ring and 2,6-diip-phenyl ring H-atom adjacent to one of the two isopropyl groups (Figure 3). It appears that the different orientation of the benzyl groups in **2** compared to that in **1** (Figure 2) makes these interactions possible in the former but not in the latter. Each of the two benzyl group phenyl rings in **2** is involved in a $\pi \cdots \pi$ interaction with another benzyl group phenyl ring (dihedral angle between the ring planes is 0°) of a neighboring molecule on one side and a C–H $\cdots \pi$ interaction with a 2,6-diip-phenyl ring H-atom from a second neighboring molecule on the other side. Similarly, two H-atoms from its two 2,6-diip-phenyl rings are involved in C–H $\cdots \pi$ interactions with the benzyl group phenyl rings of two neighboring molecules on both sides. In the $\pi \cdots \pi$ interaction, the interplanar distance and the centroid-to-centroid (Cg \cdots Cg) distance between the overlapping ring planes are 3.34 and 4.22 Å, respectively. Thus the slip angle, the angle between the normal to the planes and the Cg–Cg vector, is 37.7° [16]. In the C–H $\cdots \pi$ interaction, the H \cdots Cg and the C \cdots Cg distances are 3.171 and

4.040 Å, respectively, and the C–H...Cg angle is 156.4°. Self-assembly of **2** via these intermolecular $\pi \cdots \pi$ and C–H... π interactions leads to a two-dimensional (2-D) sheet-like structure parallel to the *bc*-plane (Figure S4 in Supplementary Material).

3.3. Spectroscopic characteristics

Infrared spectra of **1** and **2** were recorded in the range 4000–500 cm^{-1} . Both spectra display a large number of bands of various intensities (Figure S5 in Supplementary Material). In the spectra of HL¹ and HL², the N–H and the C=O stretching vibrations are at ~ 3180 and $\sim 1670 \text{ cm}^{-1}$, respectively [5]. None of the spectra of **1** and **2** displays any band in these regions. Thus during complexation, HL¹ and HL² are deprotonated and the corresponding iminolate forms (L¹)[−] and (L²)[−] are coordinated to copper in **1** and **2**, respectively (Scheme 1). Both HL¹ and HL² display a medium intensity band at $\sim 1598 \text{ cm}^{-1}$ due to the C=N stretch [5]. A similar medium intensity band observed at a slightly lower frequency of $\sim 1585 \text{ cm}^{-1}$ in the spectra of **1** and **2** is attributed to the metal coordinated C=N stretch [5, 17].

Chloroform solutions of **1** and **2** were used to record the electronic absorption spectra. The spectra of both complexes are very similar (Figure S6 in Supplementary Material). Each spectrum shows a low intensity absorption band at $\sim 560 \text{ nm}$. Similar weak absorption observed at 500–600 nm for square-planar copper(II) complexes are assigned to a d–d transition [18]. This ligand field band is followed by a moderately intense band at 395 nm and a very strong band at 280 nm. These two absorption bands are attributed to the ligand to metal charge transfer and intraligand transitions, respectively [5, 18(b,c), 19].

The X-band EPR spectra of paramagnetic **1** and **2** were recorded at room temperature (298 K) in powder phase. The spectra are illustrated in Figure 4. Both complexes display very similar axial spectra ($g_{\parallel} > g_{\perp} > 2.0023$) commonly observed for square-planar copper(II)

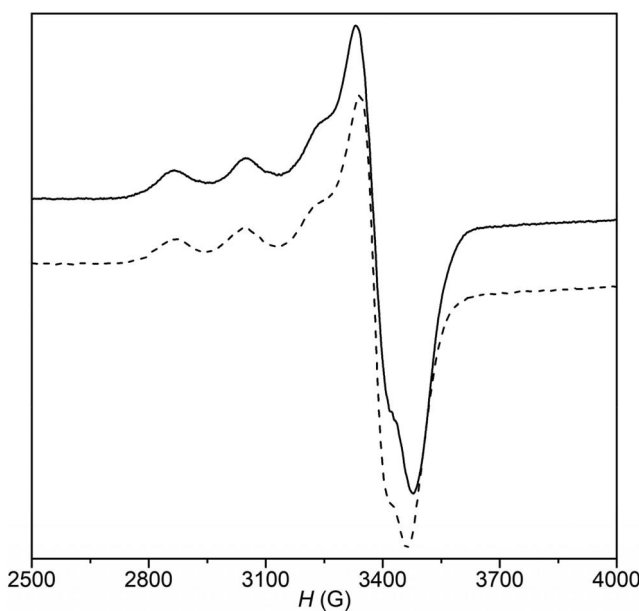


Figure 4. EPR spectra of **1** (—) and **2** (---) in powder phase at 298 K.

complexes where the unpaired electron resides in the $d_{x^2-y^2}$ orbital [18(b), 20]. The $g_{||}$, $A_{||}$, and g_{\perp} values are 2.18, 204 G, and 2.05 for **1** and 2.19, 198 G, and 2.05 for **2**. The value of $g_{||}/A_{||}$ ratio is shown as an empirical index to measure the extent of tetrahedral distortion in a square-planar copper(II) complex [20(b)]. For square-planar geometry this ratio is 105–135 cm. The $g_{||}/A_{||}$ ratio is 104 and 107 cm for **1** and **2**, respectively. Thus, the EPR spectra of both complexes are also consistent with near perfect square-planar *trans*-N₂O₂ environment around the copper(II) center in both complexes as observed in their X-ray structures.

4. Conclusion

Two copper(II) complexes, [Cu(L¹)₂] (**1**) and [Cu(L²)₂] (**2**), with the thiopseudoureas HL¹ and HL² have been synthesized and characterized. ESI mass spectrometric data and the electrically nonconducting character of the two complexes are in agreement with their molecular formulas. The X-ray crystal structures of the centrosymmetric **1** and **2** reveal the bidentate six-membered chelate ring forming iminolate-O and azomethine-N coordination mode of the ligands (L^{1/2})[−] and essentially ideal *trans*-N₂O₂ square-planar coordination geometry of the metal center in both complexes. The effective delocalization of the negative charge of (L^{1/2})[−] makes their O,N-coordination mode preferred over the O,S-coordination mode. In the solid state, the molecules of **1** and **2** are almost superimposable to each other barring the benzyl groups. As a result, intermolecular $\pi \cdots \pi$ and C–H $\cdots \pi$ interactions involving the benzyl group phenyl rings are observed in **2** but not in **1**. Due to these intermolecular noncovalent interactions, a self-assembled 2-D sheet-like structure is formed in the crystal lattice of **2**. The room temperature magnetic moment values and EPR spectra confirm the one electron paramagnetic nature and the square-planar coordination environment of the bivalent copper center (d⁹ configuration) in both **1** and **2**.

Acknowledgements

K.S. thanks the University Grants Commission (UGC), New Delhi, for a research fellowship (No. 187/ (CSIR-UGC NET June 2017). S.N. thanks the UoH-IoE for a research fellowship. G.B. thanks the UGC, New Delhi for the Dr. D.S. Kothari postdoctoral fellowship (No. F. 4-2/2006(BSR)/CH/20-21/0246).

Disclosure statement

No potential conflict of interest was reported by the authors.

Funding

Financial support to the University of Hyderabad-Institution of Eminence (UoH-IoE) from the Ministry of Education, Government of India (Grant No. F11/9/2019-U3(A)) is gratefully acknowledged.

References

- [1] (a) A. Saeed, U. Flörke, M.F. Erben. *J. Sulf. Chem.*, **35**, 318 (2014); (b) A. Saeed, R. Qamar, T.A. Fattah, U. Flörke, M.F. Erben. *Res. Chem. Intermed.*, **43**, 3053 (2017); (c) F. Steppeler, D.

- Iwan, E. Wojaczyńska, J. Wojaczyński. *Molecules*, **25**, 401 (2020);(d) U. Zahra, A. Saeed, T.A. Fattah, U. Flörke, M.F. Erben. *RSC Adv.*, **12**, 12710 (2022).
- [2] (a) V.B. Bregović, N. Basarić, K. Mlinarić-Majerski. *Coord. Chem. Rev.*, **295**, 80 (2015); (b) H.A. Nkabyo, I. Barnard, K.R. Koch, R.C. Luckay. *Coord. Chem. Rev.*, **427**, 213588 (2021);(c) A. Karmakar, S. Hazra, A.J.L. Pombeiro. *Coord. Chem. Rev.*, **453**, 214314 (2022).
- [3] (a) Y. Takemoto. *Org. Biomol. Chem.*, **3**, 4299 (2005); (b) S.J. Connon. *Chem. Commun.*, 2499 (2008);(c) K. Srinivas, P. Srinivas, P. S. Prathima, K. Balaswamy, B. Sridhar, M.M. Rao. *Catal. Sci. Technol.*, **2**, 1180 (2012);(d) Z. Zhang, P.R. Schreiner. *Chem. Soc. Rev.*, **38**, 1187 (2009);(e) O.V. Serdyuk, C.M. Heckel, S.B. Tsogoeva. *Org. Biomol. Chem.*, **11**, 7051 (2013);(f) J. Merad, J.-M. Pons, O. Chuzel, C. Bressy. *Eur. J. Org. Chem.*, **2016**, 5589 (2016).
- [4] (a) B.M. Regan, F.T. Galysh, R.N. Morris. *J. Med. Chem.*, **10**, 649 (1967); (b) T. Iwamoto, T. Watano, M. Shigekawa. *J. Biol. Chem.*, **271**, 22391 (1996);(c) T.P. Prakash, A. Püschl, M. Manoharan. *Nucleosides Nucleotides Nucleic Acids*, **26**, 149 (2007);(d) M. Ferreira, L.S. Assunção, A.H. Silva, F.B. Filippin-Monteiro, T.B. Creczynski-Pasa, M.M. Sá. *Eur. J. Med. Chem.*, **129**, 151 (2017);(e) E. Khan, S. Khan, Z. Gul, M. Muhammad. *Crit. Rev. Anal. Chem.*, **51**, 812 (2021);(f) R. Ronchetti, G. Moroni, A. Carotti, A. Gioiello, E. Camaioni. *RSC Med. Chem.*, **12**, 1046 (2021);(g) S.D. Calixto, T.L.B.V. Simão, M.V. Palmeira-Mello, G.M. Viana, P.W.M.C. Assumpção, M.G. Rezende, C.C.E. Santo, V.O. Mussi, C.R. Rodrigues, E. Lasunskiaia, A.M.T. Souza, L.M. Cabral, M.F. Muzitano. *Bioorg. Med. Chem.*, **53**, 116506 (2022) and references therein.
- [5] K. Shakunthala, A.K. Srivastava, G.N. Babu, S. Keesara, S. Pal. *Appl. Organomet. Chem.*, **35**, e6261 (2021).
- [6] D.D. Perrin, W.L.F. Armarego, D.R. Perrin. *Purification of Laboratory Chemicals*, 2nd Edn, Pergamon, Oxford (1980).
- [7] G.A. Bain, J.F. Berry. *J. Chem. Educ.*, **85**, 532 (2008).
- [8] Rigaku Oxford Diffraction Ltd., *CrysAlisPro: Data Collection and Data Processing Software*, Yarnton, England (2018).
- [9] Bruker AXS Inc., *APEX3, Program for Data Collection on Area Detectors*, Madison, Wisconsin, USA (2016).
- [10] G.M. Sheldrick. *SADABS, Program for Area Detector Absorption Correction*, University of Göttingen, Göttingen, Germany (1997).
- [11] G.M. Sheldrick. *Acta Crystallogr.*, **A64**, 112 (2008).
- [12] L.J. Farrugia. *J. Appl. Crystallogr.*, **45**, 849 (2012).
- [13] C.F. Macrae, I.J. Bruno, J.A. Chisholm, P.R. Edgington, P.McCabe, E. Pidcock, L. Rodriguez-Monge, R. Taylor, J. van de Streek, P.A. Wood. *J. Appl. Crystallogr.*, **41**, 466 (2008).
- [14] (a) C. Bolos, P.C. Christidis, G. Will, L. Wiehl. *Inorg. Chim. Acta*, **248**, 209 (1996); (b) T.I. Filyakova, L.V. Saloutina, A.Y. Zapevalov, P.A. Slepukhin, M.I. Kodess, V.I. Saloutin. *Russ. J. Org. Chem.*, **47**, 650 (2011);(c) R.K. Dani, M.K. Bharty, S.K. Kushawaha, O. Prakash, R.K. Singh, N.K. Singh. *Polyhedron*, **65**, 31 (2013).
- [15] (a) M.A.V.R. da Silva, M.D. M. C.R. da Silva, L. C.M. da Silva, J.R.B. Gomes, A.M. Damas, F. Dietze, E. Hoyer. *Inorg. Chim. Acta*, **356**, 95 (2003); (b) H. Pérez, C.C.P. da Silva, A.M. Plutín, C.A. de Simone, J. Ellena. *Acta Crystallogr. Sect. E Struct. Rep. Online*, **67**, m621 (2011);(c) S. Saeed, N. Rashid, R. Hussain, M.A. Malik, P. O'Brien, W.-T. Wong. *New J. Chem.*, **37**, 3214 (2013);(d) M. Hanif, Z.H. Chohan, J.-Y. Winum, J. Akhtar. *J. Enzyme Inhib. Med. Chem.*, **29**, 517 (2014);(e) C.T. Pham, T.H. Nguyen, K. Matsumoto, H.H. Nguyen. *Eur. J. Inorg. Chem.*, **2019**, 4142 (2019);(f) E.E. Oyeka, I. Babahan, B. Eboma, K.J. Ifeanyieze, O.C. Okpareke, E.P. Coban, A. Özmen, B. Coban, M. Aksel, N. Özdemir, T.V. Groutso, J.I. Ayogu, U. Yildiz, M.D. Bilgin, H.H. Biyik, B.R. Schrage, C.J. Ziegler, J.N. Asegbeloyin. *Inorg. Chim. Acta*, **528**, 120590 (2021);(g) K.I.Y. Ketchemen, M.D. Khan, S. Mlowe, M.P. Akerman, I. Vitorica-Yrezabal, G. Whitehead, L.D. Nyamen, P.T. Ndifon, N. Revaprasadu, P. O'Brien. *J. Mol. Struct.*, **1229**, 129791 (2021);(h) C.M. Leite, J. Honorato, A.C.B.M. Martin, R.G. Silveira, F.M. Colombari, J.C. Amaral, A.R. Costa, M.R. Cominetti, A.M. Plutín, D. de Aguiar, B.G. Vaz, A.A. Batista. *Inorg. Chem.*, **61**, 664 (2022).

- [16] N.R. Sangeetha, S.N. Pal, C.E. Anson, A.K. Powell, S. Pal. *Inorg. Chem. Commun.*, **3**, 415 (2000).
- [17] (a) S. Das, S. Pal. *J. Organomet. Chem.*, **691**, 2575 (2006); (b) R. Raveendran, S. Pal. *Inorg. Chim. Acta*, **359**, 3212 (2006); (c) A. Mukhopadhyay, S. Pal. *Eur. J. Inorg. Chem.*, **2009**, 4141 (2009); (d) A.R.B. Rao, S. Pal. *J. Organomet. Chem.*, **731**, 67 (2013); (e) T. Ghosh, S. Pal. *J. Chem. Sci.*, **127**, 1201 (2015).
- [18] (a) Z.D. Matović, V.D. Miletic, G. Samardžić, G. Pelosi, S. Ianelli, S. Trifunović. *Inorg. Chim. Acta*, **358**, 3135 (2005); (b) E. Faggi, R. Gavara, M. Bolte, L. Fajarí, L. Juliá, L. Rodríguez, I. Alfonso. *Dalton Trans.*, **44**, 12700 (2015); (c) G. Sciortino, J.-D. Maréchal, I. Fábíán, N. Lihi, E. Garribba. *J. Inorg. Biochem.*, **204**, 110953 (2020).
- [19] (a) T. Ghosh, A. Mukhopadhyay, K.S.C. Dargaiah, S. Pal. *Struct. Chem.*, **21**, 147 (2010); (b) T. Ghosh, S. Pal. *Inorg. Chim. Acta*, **363**, 3632 (2010).
- [20] (a) J. Peisach, W.E. Blumberg. *Arch. Biochem. Biophys.*, **165**, 691 (1974); (b) U. Sakaguchi, A.W. Addison. *J. Chem. Soc., Dalton Trans.*, 600 (1979); (c) E. Garribba, G. Micera. *J. Chem. Educ.*, **83**, 1229 (2006); (d) S. Das, S.A. Maloor, S.N. Pal, S. Pal. *Cryst. Growth Des.*, **6**, 2103 (2006).